Microchimica Acta (2021) 188: 68
https://doi.org/10.1007/s00604-020-04678-w

ORIGINAL PAPER

Electrochemiluminescence biosensor for microRNA determination based on AgNCs@MoS_2 composite with (AuNPs-Semicarbazide)@Cu-MOF as coreaction accelerator

Fei Li[1] · Minghui Wang[2] · Yunlei Zhou[1] · Huanshun Yin[1] · Shiyun Ai[1]

Received: 16 September 2020 / Accepted: 1 December 2020 / Published online: 5 February 2021

Abstract

A novel electrochemiluminescence (ECL) biosensor was fabricated for miRNA-162a detection by using silver nanoclusters/molybdenum disulfide (AgNCs@MoS_2) as an ECL material, peroxodisulfate ($S_2O_8^{2-}$) as a co-reactant, and semicarbazide (Sem) as a co-reaction accelerator. Firstly, hairpin probe H_a modified on AgNCs@MoS_2/GCE was unfolded based on its hybridization with target microRNA. Then, the unfolded H_a can further be hybridized with another hairpin DNA of H_b on (AuNPs-semicarbazide)@Cu-MOF, resulting in the release of target microRNA, which further causes a cyclic hybridization. This creates more (AuNPs-semicarbazide)@Cu-MOF on the electrode surface, achieving cyclic hybridization signal amplification. Strikingly, due to the presence of Sem, accelerating the reduction of $S_2O_8^{2-}$ and resulting in the generation of more oxidant intermediates of SO_4^{2-}, the amount of excited states of Agincreases to further amplify the ECL signal. The biosensor exhibited high sensitivity with a low LOD of 1.067 fM, indicating that the introduction of co-reaction accelerators can provide an effective method for signal amplification. The applicability of this method was assessed by investigating the effect of Pb(II) ion on miRNA-162a expression level in maize seedling leaves.

Keywords MicroRNA · Co-reaction accelerator · AgNCs@MoS_2 · Electrochemiluminescence · (AuNPs-Semicarbazide)@Cu-MOF

Introduction

MicroRNAs (miRNAs) are an extensive class of ~22-nucleotide noncoding and small RNAs that function as ubiquitous post-transcriptional regulators of gene expression in plants and animals [1]. It is crucial for the control of animal and plant development and physiology and plays an important role in cell cycle, differentiation, development, and metabolism [2–5]. Previous research has demonstrated that miRNAs involved in various plant biological processes, such as leaf and root development, flowering, and ripe fruit and various stress responses [6]. However, due to its small size, low content, high sequence similarity, and easy degradation, it makes miRNA detection very challenging. Strikingly, various analytical methods have been developed, including northern blotting analysis, microarrays, and real-time quantitative PCR detection [7–9]. Although most of them are convenient and reliable, the sensitivity and specificity of these methods are not satisfactory (detailed information compared in Table S1). Therefore, a simple, convenient, low-cost, and ultra-sensitive method for miRNA detection is desirable.

So far, several promising miRNA detection strategies have been explored, including electrochemical [10, 11], colorimetric [12], fluorescent [13–15], photoelectrochemical (PEC) [16–18], and electrochemiluminescence (ECL) [19–21]. Compared with other optical methods, ECL shows its potential advantages through the intelligent integration of electrochemistry and spectroscopy. Noteworthy, Zhong et al. [22] constructed an ECL biosensor based on self-catalytic CDs-

Fei Li and Minghui Wang contributed equally to this work.

✉ Yunlei Zhou
zhyl@sdau.edu.cn

[1] Food Safety Analysis and Test Engineering Technology Research Center of Shandong Province, College of Chemistry and Material Science, Shandong Agricultural University, Taian 271018, People's Republic of China

[2] State Key Laboratory of Pharmaceutical Biotechnology, School of Life Sciences, Nanjing University, Nanjing 210023, People's Republic of China

Au-PEI@TiO_2 nanoparticles and target-triggered CHA and successfully realized the sensitive detection of miRNA-21. The detection limit of the constructed sensor is 0.03 fM, and it also shows good results in actual sample applications. In addition, Shao et al. [23] designed a ruthenium-based metal organic framework (Ru-MOF) as a signal unit electrochemiluminescence biosensor to detect miRNA-141. The selectivity, stability, reproducibility, precision, and application were validated and offer a new perspective and method for tumor marker detection. Therefore, based on the advantages of high sensitivity, low background signal, wide linear range, controllable electrochemical potential, and good selectivity, ECL biosensors have aroused great interest, and they are widely used for the detection of various biomolecules. Naturally, ECL is also a potentially excellent platform for sensitive detection of miRNA and shows great advantage and value in basic research and early clinical diagnosis in the future.

However, with the development of science and technology, higher requirements have been placed on existing ECL analysis methods. As we all know, in ECL sensors, selection of luminescent nanomaterials is one of the important factors affecting ECL performance. Recently, metal clusters (NCs), as a kind of self-luminous nanomaterials with electrochemiluminescence activity, have received widespread attention [24, 25]. Due to the size and property of nanoclusters between a single atom and nanoparticle, their optical property, chemical properties, and electrical property are significantly different from a single atom and large nanoparticle. More importantly, due to the existence of quantum confined effect, nanocluster exhibits an excellent optical property [26]. As a kind of precious metal cluster, AgNCs can be used as a new type of light-emitting reagent for future ECL biosensors due to their good water solubility, low toxicity, inexpensive, and excellent stability [27, 28].

In recent years, due to its excellent electrical, electrochemical, optical, and other properties, two-dimensional MoS_2 nanosheets have been widely used in various aspects such as optoelectronic devices, field effect transistors, sensors, and biomedicine through different modifications and doping modifications. Molybdenum disulfide (MoS_2) is a non-toxic and environmentally friendly two-dimensional (2D) transition metal disulfide. Considering that the morphology and size of the electrode material are related to its electrochemical performance, MoS_2 with different morphologies has been successfully synthesized. In terms of electrical performance, for thin layer MoS_2, the band gap can reach about 1.8 eV, so layered MoS_2 is currently widely used to prepare low-power electronic devices and other semiconductor power devices. In addition, due to their excellent electrical conductivity, biocompatibility, and large specific surface area, MoS_2 show unique advantages in the construction of ECL biosensors. Therefore, not only the excellent electrical conductivity of MoS_2 is used as the base material of ECL, but also the large specific surface area of MoS_2 is used to load a large number of AgNCs.

Another, it is important to amplify detection signal to improve the performance of ECL biosensors for detecting the expression level of miRNA. As a simple and effective strategy, the co-reactant attracts more attentions, which can effective amplify the ECL signal, such as $S_2O_8^{2-}$ and trimethylamine. In general, $S_2O_8^{2-}$ is transformed into $SO_4^{\bullet-}$ by electrochemical reduction, and the produced $SO_4^{\bullet-}$ can be excited by injecting holes into the highest occupied molecular orbital, thereby reacting with negatively charged molecules, leading to ECL intensity significantly enhanced [29, 30]. The stronger ECL response can be produced with generating more $SO_4^{\bullet-}$. Therefore, the increasing co-reactant amount to achieve signal amplification is a problem that needs to be solved urgently. However, due to the limited solubility of $S_2O_8^{2-}$ and the non-absolutely linear relationship between the concentration of $S_2O_8^{2-}$ and the amount of $SO_4^{\bullet-}$, it is restricted to improve the ECL intensity by increasing the concentration of $S_2O_8^{2-}$. To solve it, Ma et al. [31] proposed the concept of co-reaction accelerators, that is, a class of substance that have a promoting effect on the ECL co-reaction system, which can accelerate the reduction of $S_2O_8^{2-}$ to generate more $SO_4^{\bullet-}$, thereby further increasing the generation of the excited state of the molecule to emit light. Based on it, Sun et al. [32] designed a new near-infrared electrochemiluminescence resonance energy transfer strategy for enzyme-free amplified DNA detection that used semicarbazide (Sem) as a co-reaction accelerator to promote the ECL reaction rate of Cu-Zn-In-S NCs and the $S_2O_8^{2-}$ system for significantly boosting the ECL intensity. Noteworthy, semicarbazide (Sem) is a co-reaction accelerator, which can greatly promote the reaction between ECL probe and co-reaction, increasing the ECL intensity [33]. This means that the synergistic reaction accelerator can increase the ECL reaction rate of the co-reactant and the luminophore. Sem could accelerate the reduction of $S_2O_8^{2-}$, resulting in the generation of more oxidant intermediates of $SO_4^{\bullet-}$, the amount of excited states of luminophor could be increased to further amplify the ECL signal. Therefore, the introduction of co-reaction promoters can provide an effective method for signal amplification; this will be a potential signal amplification strategy for the development of biosensor.

Experimental section

Regents and instruments

The used reagents and instruments, the synthesis process for Cu-MOF, AgNCs@MoS_2, and H_b-(AuNPs-Sem)@Cu-MOF were introduced in Supplementary Material.

Biosensor fabrication

The bare GCE electrode ($d = 3$ mm) was firstly polished to obtain a mirror-like surface using a 0.3-μm Al_2O_3 slurry. Then, the GCE was washed with deionized water and ethanol for 3 times. After dried under N_2 blowing, 10 μL of 1.5 mg/mL AgNCs@MoS_2 dispersion was casted onto GCE, which was dried under the irradiation of infrared lamp. The prepared electrode was noted as AgNCs@MoS_2/GCE. Subsequently, 10 μL of probe immobilization buffer containing 0.1 μM hairpin DNA probe (H_a) was dropped onto the electrode, which was incubated for 4 h at room temperature under humid condition. This prepared electrode was labeled DNA/AgNCs@MoS_2/GCE. After that, 10 μL of different concentrations of the target miRNA was added dropwise onto the electrode and incubated at 37 °C for 2 h under humid conditions. The electrode was labeled DNA-RNA/AgNCs@MoS_2/GCE. Finally, 10 μL of 1× DNA hybridization buffer containing H_b-(AuNPs-Sem)@Cu-MOF solution was added dropwise to the above electrode surface and reacted for 2 h in a moist environment at 37 °C. This electrode was labeled H_b-(AuNPs-Sem)@Cu-MOF/DNA-RNA/AgNCs@MoS_2/GCE. Between each modification process, the prepared electrode was rinsed with washing buffer. The modified electrode was immersed in 10 mL of detection solution for detection, the voltage scan range was − 2–0 V, the scan rate: 100 mV/s, and the photomultiplier tube: 900 V.

Results and discussion

Detection strategy

A signal-on ECL biosensor was fabricated based on AgNCs@MoS_2 as electroluminescent materials, $S_2O_8^{2-}$ as a co-reaction reagent, and semicarbazide (Sem) as a co-reaction promoter. The detection mechanism is shown in Scheme 1. First, MoS_2 nanosheets were prepared by the hydrothermal method, and then, the light-emitting active material of AgNCs were in situ reduced on MoS_2 nanosheet surface to prepare AgNCs@MoS_2, which was employed as a light-emitting nanocomposite. Then, H_b-(AuNPs-Sem)@Cu-MOF composite was prepared as an ECL co-reaction accelerator. To construct the ECL biosensor, the hairpin probe H_a was assembled on the AgNCs@MoS_2/GCE surface through the interaction of Ag with the –SH at the 3′-terminal of probe H_a. At this state, the hairpin probe DNA H_a was closed. However, when target miRNA was introduced, the hairpin probe DNA H_a was unfolded and the fragment at its 5′-terminal kept un-hybridization. Afterwards, the un-hybridized sequence of H_a was further hybridized with H_b, making the (AuNPs-Sem)@Cu-MOF composite immobilized on the electrode surface to improve the ECL signal. Moreover, the hybridized miRNA can be gradually released to execute another hybridization with H_a, achieving a circulation hybridization. As a result, a low amount of target miRNA can lead to immobilize more (AuNPs-Sem)@Cu-MOF on the electrode surface, realizing the cyclic hybridization signal amplification.

Herein, Sem in the (AuNPs-Sem)@Cu-MOF is a co-reaction accelerator that can make the co-reactant $S_2O_8^{2-}$ produce more active substances $SO_4^{\bullet-}$, which further boosted the production of excited states of AgNCs to emit light. It is reported that the larger the amount of the $SO_4^{\bullet-}$ were produced, the stronger the ECL response of the NCs could be achieved. According to the literature, the possible luminescence mechanism of AgNCs in the presence of co-reactant $S_2O_8^{2-}$ is as follows [34]:

$$AgNCs + e^- \rightarrow AgNCs^-$$
$$S_2O_8^{2-} + e^- \rightarrow SO_4^{\bullet-} + SO_4^{2-}$$
$$S_2O_8^{2-} + e^- \rightarrow SO_4^{\bullet-} + SO_4^{2-}$$
$$AgNCs^* \rightarrow AgNCs + h\nu$$

AgNCs and $S_2O_8^{2-}$ simultaneously acquire one electron to produce $AgNCs^-$ and $SO_4^{\bullet-}$ intermediates. $AgNCs^-$ and $SO_4^{\bullet-}$ further interact to generate excited-state AgNCs*, which releases energy for luminescence, thereby returning to the ground state. The schematic illustration of the ECL biosensor preparation process and possible luminescence mechanism has been shown in Scheme 1. Obviously, the addition of Sem increases the ECL signal of AgNCs and Sem is likely to react with the co-reactant $K_2S_2O_8$ instead of the luminophore AgNCs as follows [31]:

$$Sem - e^- \rightarrow Sem^{\bullet+} \rightarrow Sem^{\bullet} + H^+$$
$$Sem^{\bullet} + S_2O_8^{2-} \rightarrow Sem^+ + SO_4^{\bullet-}$$

Sem loses electrons and is oxidized and further generates $Sem^{\bullet}$ through deprotonation, and then interacts with $K_2S_2O_8$ to produce more $SO_4^{\bullet-}$ for AgNC to luminescence.

Among them, Cu-MOF can provide a large surface area for Sem loading, and the large amount of Sem introduced greatly enhanced the ECL signal of the co-reaction system. As the concentration of miRNA increases, the more (AuNPs-Sem)@Cu-MOF is introduced, and the stronger ECL signal of the sensor is achieved. Therefore, based on the relationship between miRNA concentration and ECL signal, miRNA can be detected.

Characterization of materials

The MoS_2 nanosheets were characterized by SEM, XRD, and Raman spectroscopy. The corresponding description was represented in the Supplementary Material. From the TEM of AgNCs@MoS_2 (Fig. 1a), it can be seen that the particle size of the nanosilver cluster is about 5 nm and is evenly loaded on

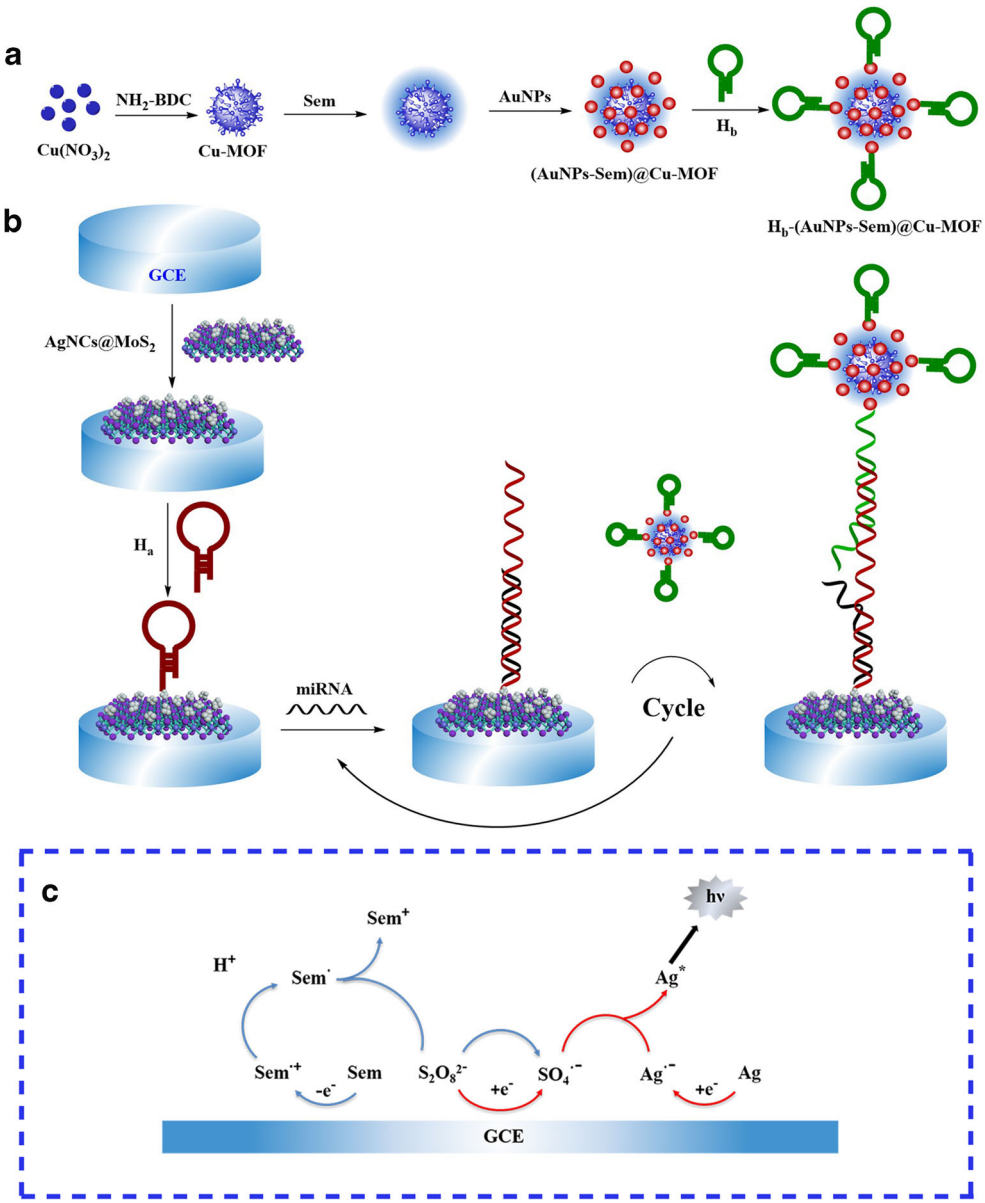

Scheme 1 **a** Fabrication of H_b-(AuNPs-Sem)@Cu-MOF composite. **b** Schematic illustration of the preparation of ECL biosensor. **c** Possible mechanism for the ECL system.

the MoS_2 nanosheets. Through EDS mapping (Fig. 1b), it can be seen that the Mo, S, and Ag elements are evenly distributed, which further proves the successful preparation of AgNCs@MoS_2. In addition, the prepared Cu-MOF was characterized by SEM and FT-IR. Figure 1c presented the SEM image of Cu-MOF with a cube structure. The particle size is about 300 nm. The FT-IR spectra of Cu-MOFs were shown in Fig. 1d. Notably, the absorption peaks of 3230 and 2937 cm^{-1} belonged to stretching vibration of the N-H bond in the $–NH_2$ [35]. The peaks at 1613 cm^{-1} and 1371 cm^{-1} was attributed to C-O (carboxy) asymmetric stretching and asymmetric bending vibrations; the peak at 3412 cm^{-1} was ascribed to the O-H group (carboxy) stretching vibration, which demonstrated the existence of the -COOH and -OH groups in Cu-MOFs. In addition, several absorption bands at 1089 and 1412 cm^{-1} were ascribed to the C-O-C and C-N stretching or bending vibrations, respectively [36, 37]. It further testified that Cu-MOFs had been prepared successfully.

Characterization of the modified electrodes

The fabrication process of the biosensor was monitored by EIS in 5 mM $[Fe(CN)_6]^{3-/4-}$ (1 : 1) solution containing 0.1 M KCl with the frequency range from 10^{-1} to 10^5 Hz. The results were illustrated in Fig. 2a. The bare electrode (curve A) exhibited a small semicircle in the high-frequency region, indicating a low interfacial electron transfer resistance (R_{et}). When AgNCs@MoS_2 was fixed on the electrode surface (curve B), the R_{et} value was enhanced. It can be attributed to the negative charge on the surface of MoS_2, which inhibited

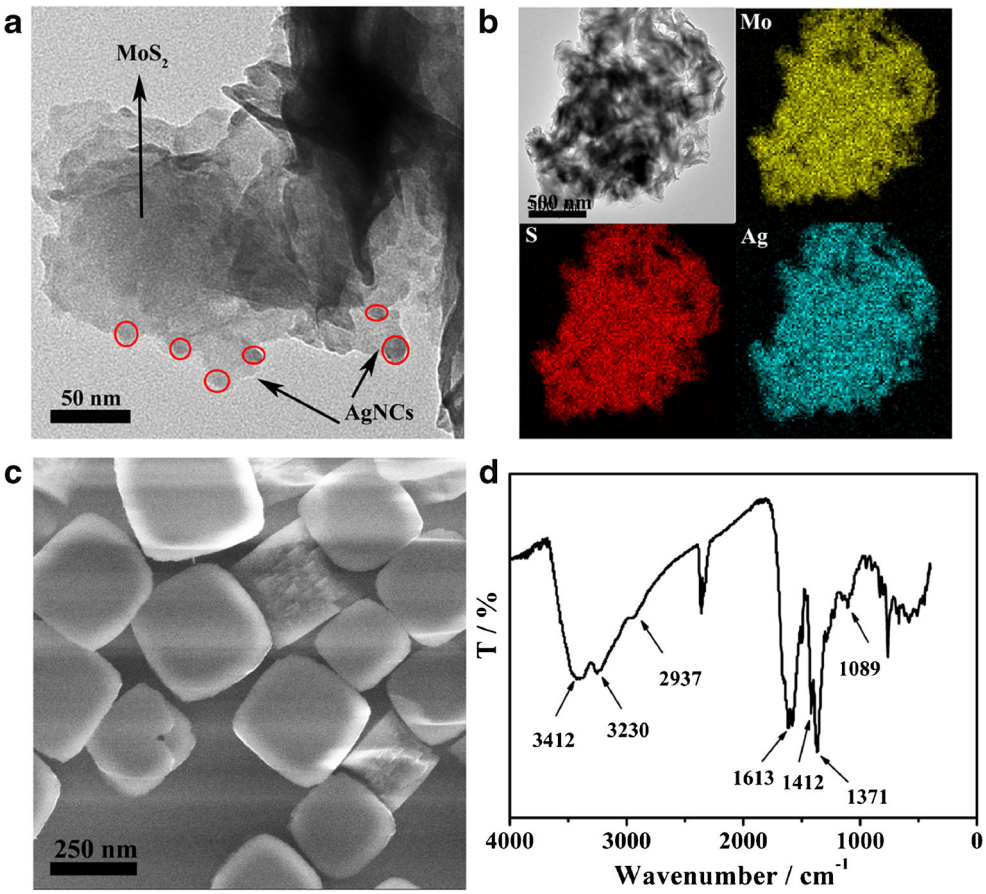

Fig. 1 **a** TEM image of AgNCs@MoS_2. **b** TEM image and the EDS mapping of AgNCs@MoS_2. **c** SEM image of Cu-MOF. **d** FT-IR spectrum of Cu-MOF

the diffusion of a electronegative redox probe. When the hairpin probe (H_a) (curve C) and miRNA (curve D) were sequentially assembled on the electrode surface, the impedance increased gradually, which was caused by the electrostatic repulsion between the negatively charged phosphate backbone on the nucleic acid and the redox probe. The introduction of H_b-(AuNPs-Sem)@Cu-MOF (curve E) further hindered the electron transfer, leading to the further increase of the R_{et} due to the large volume and poor conductivity of Cu-MOF preventing the diffusion of $[Fe(CN)_6]^{3-/4}$. The impedance change before and after the electrode modification indicates the successful modification of the electrode.

To verify the feasibility of the developed method for miRNA detection, the ECL response of various modified electrodes were measured and compared. As seen in Fig. 2b, the AgNCs@MoS_2/GCE electrode (curve A) showed an initial and stable response, indicating that AgNCs@MoS_2 composites possess good luminous performance. When H_a (curve B)

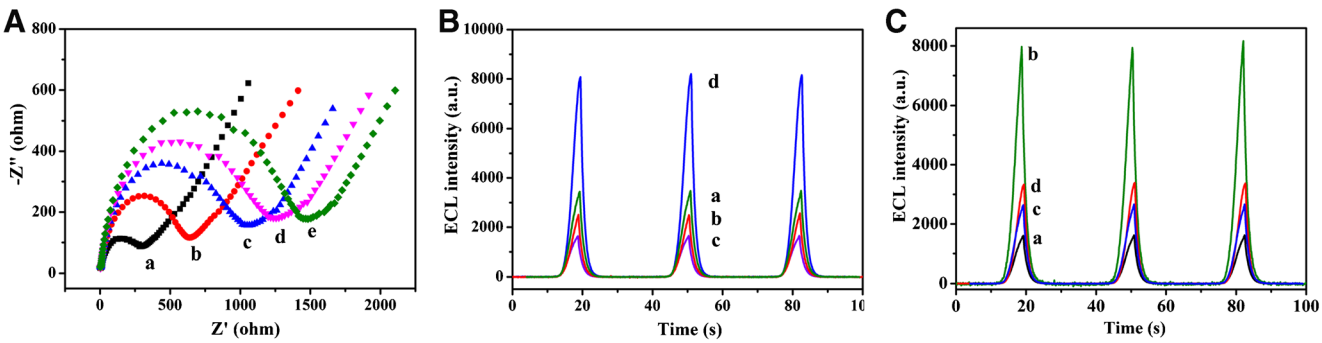

Fig. 2 **a** The Nyquist plot of the bare GCE (**A**), AgNCs@MoS_2/GCE (**B**), DNA/AgNCs@MoS_2/GCE (**C**), DNA-RNA/AgNCs@MoS_2/GCE (**D**), and H_b-(AuNPs-Sem)@Cu-MOF/DNA-RNA/AgNCs@MoS_2/GCE (**E**). **b** ECL intensity of AgNCs@MoS_2/GCE (**A**), DNA/AgNCs@MoS_2/GCE (**B**), DNA-RNA/AgNCs@MoS_2/GCE (**C**), and H_b-(AuNPs-Sem)@Cu-MOF /DNA-RNA/AgNCs@MoS_2/GCE (**D**). **c** DNA-RNA/AgNCs@MoS_2/GCE (**A**), H_b-(AuNPs-Sem)@Cu-MOF/DNA-RNA/AgNCs@MoS_2/GCE (**B**), H_b-AuNPs@Cu-MOF/DNA-RNA/AgNCs@MoS_2/GCE (**C**), and H_b-(AuNPs-Sem) /DNA-RNA/AgNCs@MoS_2/GCE (**D**)

and miRNA (curve C) were successively modified on the electrode, the ECL intensity was further decreased, which is an attribute to the reduction of electron transfer efficiency due to the steric hindrance of nucleotides. However, when H_b-(AuNPs-Sem)@Cu-MOF was further modified on the electrode surface, the ECL intensity improved significantly (curve D). It can be greatly attributed to semicarbazide, which can be seen in Fig. 2c. In Fig. 2c, the role played by Sem and Cu-MOF in the sensor were further verified through experiments. The ECL response intensity of curve B is significantly higher than curve c; it is indicated that Sem plays a vital role in signal amplification in the sensor process and can be an excellent signal amplification technology. In addition, the ECL response intensity of curve B is significantly higher than that of curve D, which is mainly due to the larger specific surface area of Cu-MOF, which can load a large amount of Sem and probe H_b to achieve the purpose of increasing signal specificity. Therefore, when only Sem and Cu-MOF exist at the same time, ECL signal is the strongest, which proves that they are an indispensable part of the sensor and play an important role in signal amplification. These results also confirm the detection feasibility of the developed method.

Optimization of assay conditions

The following parameters were optimized: MoS_2 concentration (A), H_a concentration (B), miRNA hybridization time (C), and H_b hybridization time (D). Respective data and figures (Fig. S2) are given in the Electronic Supplementary Material. The optimal condition obtained by the experiment is the MoS_2 concentration of 1.5 mg/mL, H_a concentration of 0.1 μM, miRNA hybridization time of 100 min, and H_b hybridization time of 120 min.

Detection performance

To testify the analytical performance of the biosensor, the ECL intensity of different concentrations of miRNA-162a was measured and compared. As shown in Fig. 3a, under optimal experimental conditions, the ECL intensity enhanced when increasing miRNA-162a concentration from 10 to 5000 fM. In this detection range, the logarithmic value of miRNA-162a concentration is linear with the ECL intensity. The linear regression equation is $I_{ECL} = 1434\log c\ (\mathrm{fM}) + 2517$ and the linear correlation coefficient $R = 0.9948$ (Fig. 3b). The detection limit was calculated to be 28.1 aM (3σ) (detail in Supplementary Material). Compared with previous work, as listed in Table 1, this experiment shows certain advantages and attractiveness. (1) Firstly, ECL technique possesses the advantages of weak background interference, miniaturization of the instrument, and simple operation method. (2) Secondly, this ECL biosensor exhibited a reasonable linear range and low detection limit. (3) The ECL material employed is MoS_2@AgNCs, which has excellent electrical conductivity and luminescence properties and has a certain attractiveness. Moreover, using semicarbazide as a co-reaction promoter to promote the ECL reaction rate between the luminophore AgNCs and its co-reactant ($S_2O_8^{2-}$) for signal amplification,

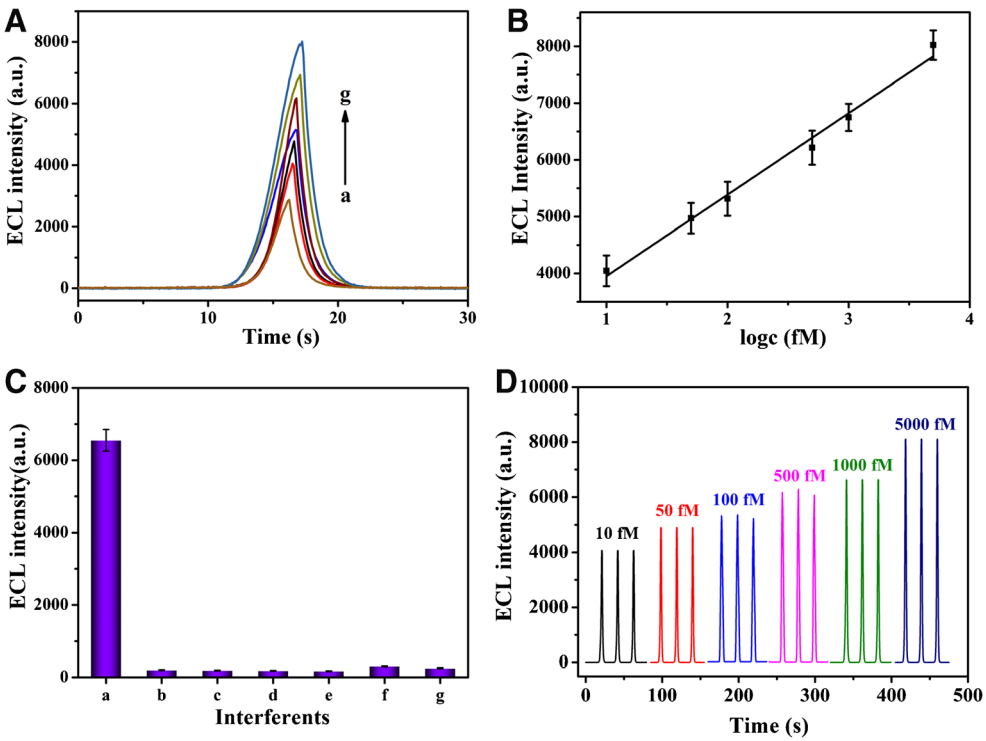

Fig. 3 **a** ECL response of the biosensor with different concentrations of miRNA-162a. **A**–**G** 0, 10, 50, 100, 500, 1000, and 5000 fM. **b** The linear relationship between the ECL intensity and the logarithm value of miRBA-162a concentration. **c** The histogram for the ECL intensity of the biosensor fabricated with various miRNAs. **A** miRNA-162a, **B** miRNA-156d, **C** miRNA-169a, **D** miRNA-166e, **E** miRNA-172a, **F** single-base mismatched miRNA, and **G** three-base mismatched miRNA. The concentration of miRNA is 5000 fM. **d** Continuous cyclic potential scans of the ECL biosensor. The voltage of the photomultiplier tube in the whole experiment is 900 V

Table 1 Comparison of detection performance for miRNA detection

Method	Linear range (pM)	Detection limit (pM)	Electrode construction time (h)	Recovery (%)	RSD (%)	Refs.
Electrochemistry	0.001–1000	4×10^{-4}	13	97.5–103.2	–	[38]
Fluorescence	0.01–10	7.3×10^{-3}	–	–	–	[39]
PEC	0.001–10	5×10^{-4}	16	90–103.3	2.1–6.3	[40]
ECL	0.1–100	3.3×10^{-2}	4	–	–	[41]
ECL	0.05–100,000	5×10^{-2}	21–25	–	–	[42]
ECL	0.01–5	1.07×10^{-3}	8	96.49–108.33	3.12–5.1	This work

the signal amplification strategy has a certain novelty. (4) The applicability of this method was testified by investigating the effect of heavy metal on the expression of miRNA content in maize seedling leaves.

Selectivity is one of the critical factors for the performance of a biosensor. To verify the selectivity of the method, we selected miRNA-156d, miRNA-169a, miRNA-166e, miRNA-172a, single-base mismatched miRNA, and three-base mismatched miRNA as interferences to evaluate the sensor selectivity. To perform it, the change of the ECL intensity ($\Delta ECL = ECL_1 - ECL_2$) of the biosensor was compared, where ECL_1 was the ECL intensity of DNA/AgNCs@MoS_2/GCE incubated with different miRNAs and H_b-(AuNPs-Sem)@Cu-MOF as described in "Reagents and instruments," ECL_2 was the ECL intensity of DNA/AgNCs@MoS_2/GCE. As illustrated in Fig. 3c, the ΔECL for miRNA-162a was greatly higher than other miRNAs, indicating that the fabricated biosensor can distinguish the target miRNA-162a from other miRNAs. The result proved the remarkable selectivity of the biosensor.

Stability is an important parameter for the biosensor, so it was also assessed. The ECL intensity of the biosensor had no significant change under 10 continuous cyclic scans (RSD = 0.85%, Fig. 3d). The above result indicated that the biosensor had superior stability.

Detection of miRNA-162a in samples

With the development of society, more and more pollutants enter the environment, causing increasingly serious environmental pollution and food security problems. Heavy metal pollution is currently one of the severe environmental pollution problems in the world. Plumbum (Pb), as one of the important toxic heavy metal elements, has become a major environmental problem threatening ecological security and food security, and it has three causes (carcinogenic, teratogenic, and mutagenic) to organisms. Excessive Pb will have a certain effect on the growth of plants, and its effects include reduced plant germination rate, poor growth, and reduced fruits. At the same time, it can accumulate in plants through plant roots and can enter humans and animals through the food chain to endanger their health. miRNAs play a crucial role in plant growth and development. miRNA is also involved in plant stress pathway, such as salt stress [43–45]. Thus, to investigate the practical applicability of this method, miRNA-162a content in the genomic RNA of maize seedling leaves treated with different concentrations of heavy metal ions (Pb^{2+}) was measured by this biosensor. As shown in Fig. 4, the expression level of miRNA-162a enhanced with increasing Pb^{2+} concentration, indicating that Pb(II) ion can affect miRNA expression, which may affect plant growth and development. To testify the accurateness of the biosensor, the detection results were also compared with that by qRT-PCR technology. As illustrated in Fig. 4, almost no significant difference was obtained in the results of the two methods, indicating the superior practicability of the biosensor. This quick and easy method can help researchers better understand the miRNA regulatory network and may provide a new marker for the evaluation of the ecotoxicological effects of Pb^{2+} pollutants towards plants.

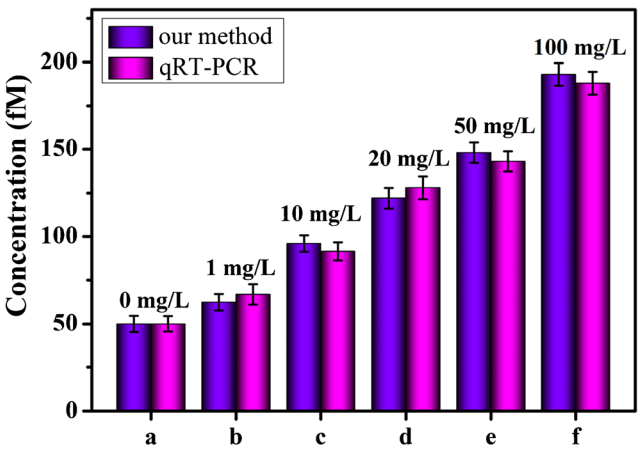

Fig. 4 Influence of various concentrations of Pb^{2+} on miRNA-162a expression in maize seedling leaves

Conclusions

A sensitive ECL biosensor was fabricated for miRNA-162a detection, where semicarbazide was employed as the co-reaction accelerator to promote the ECL reaction rate of AgNCs, and peroxydisulfate ($S_2O_8^{2-}$) was used as the co-reactant for boosting signal amplification. This biosensor platform shows attractive features: (i) the AgNCs@MoS_2 composite exhibited excellent electron transmission characteristics and large specific surface area, making it a promising candidate for the development of ECL biosensors and (ii) Cu-MOFs are used as the carrier of semicarbazide, and a large amount of semicarbazide is introduced into the sensor to act as a novel ECL co-reaction accelerator for signal amplification. Due to the above merits, this method presents acceptable analytical performance. Moreover, the effect of heavy metal on miRNA-162a content in maize leaves was successfully assessed, indicating the potential applicability of this method. However, the detection of miRNA in genome and in vivo is still insufficient in this work. Further optimizing the construction time of the sensor, and realizing the detection of miRNA in vivo, and realizing the detection of miRNA more quickly and efficiently will be the most important work in the future.

Supplementary Information The online version contains supplementary material available at https://doi.org/10.1007/s00604-020-04678-w.

Acknowledgments This work was supported by the Natural Science Foundation of Shandong Province of China (No. ZR2018MB028), Science and Technology Support Plan for Youth Innovation of Colleges and Universities of Shandong (2019KJC019), and National Natural Science Foundation of China (Nos. 21775090 and 41807484).

Compliance with ethical standards

Conflict of interest The authors declare that they have no conflicts of interest.

References

1. Bose D, Jayaraj GG, Kumar S, Maiti S (2013) A molecular-beacon-based screen for small molecule inhibitors of miRNA maturation. ACS Chem Biol 8(5):930–938. https://doi.org/10.1021/cb300650y
2. Jia H, Li Z, Liu C, Cheng Y (2010) Ultrasensitive detection of microRNAs by exponential isothermal amplification. Angew Chem Int Edit 49(32):5498–5501. https://doi.org/10.1002/anie.201001375
3. Yang GD, Li YY, Wu BJ, Zhang KY, Gao L, Zheng CC (2019) MicroRNAs transcriptionally regulate promoter activity in Arabidopsis thaliana. J Integr Plant Biol 61(11):1128–1133. https://doi.org/10.1111/jipb.12775
4. Su YH, Liu YB, Zhou C, Li XM, Zhang XS (2016) The microRNA167 controls somatic embryogenesis in Arabidopsis through regulating its target genes ARF6 and ARF8. Plant Cell Tiss Org 124(2):405–417. https://doi.org/10.1007/s11240-015-0903-3
5. Wu L, Liu DF, Wu JJ, Zhang RZ, Qin ZR, Liu DM, Li AL, Fu DL, Zhai WX, Mao L (2013) Regulation of FLOWERING LOCUS T by a microRNA in Brachypodium distachyon. Plant Cell 25(11):4363–4377. https://doi.org/10.1105/tpc.113.118620
6. Zhang X, Li K, Xing R, Liu S, Chen X, Yang H, Li P (2018) MiRNA and mRNA expression profiles reveal insight into chitosan-mediated regulation of plant growth. J Agr Food Chem 66(15):3810–3822. https://doi.org/10.1021/acs.jafc.7b06081
7. Ouyang T, Liu Z, Han Z, Ge Q (2019) MicroRNA detection specificity: recent advances and future perspective. Anal Chem 91(5):3179–3186. https://doi.org/10.1021/acs.analchem.8b05909
8. Dong H, Lei J, Ding L, Wen Y, Ju H, Zhang X (2013) MicroRNA: function, detection, and bioanalysis. Chem Rev 113(8):6207–6233. https://doi.org/10.1021/cr300362f
9. Hunt EA, Broyles D, Head T, Deo SK (2015) MicroRNA detection: current technology and research strategies. Annu Rev Anal Chem 8(1):217–237. https://doi.org/10.1146/annurev-anchem-071114-040343
10. Xu J, Yan C, Wang X, Yao B, Lu J, Liu G, Chen W (2019) Ingenious design of DNA concatamers and G-quadruplex wires assisted assembly of multibranched DNA nanoarchitectures for ultrasensitive biosensing of miRNA. Anal Chem 91(15):9747–9753. https://doi.org/10.1021/acs.analchem.9b01353
11. Akbarnia A, Zare HR (2018) A voltammetric assay for microRNA-25 based on the use of amino-functionalized graphene quantum dots and ss- and ds-DNAs as gene probes. Microchim. Acta 185(11):503. https://doi.org/10.1007/s00604-018-3037-6
12. Lee J, Kim Y-k, Lee S, Yoon S, Kim W-k (2019) Graphene oxide-based NET strategy for enhanced colorimetric sensing of miRNA. Sensor Actuat B-Chem 282:861–867. https://doi.org/10.1016/j.snb.2018.11.149
13. Chen X, Xu K, Li J, Yang M, Li X, Chen Q, Lu C, Yang H (2020) Switch-conversional ratiometric fluorescence biosensor for miRNA detection. Biosens Bioelectron 155:112104. https://doi.org/10.1016/j.bios.2020.112104
14. Cao X, Zhang K, Yan W, Xia Z, He S, Xu X, Ye Y, Wei Z, Liu S (2020) Calcium ion assisted fluorescence determination of microRNA-167 using carbon dots–labeled probe DNA and polydopamine-coated Fe_3O_4 nanoparticles. Microchim Acta 187(4):212. https://doi.org/10.1007/s00604-020-4209-8
15. Wu H, Wang H, Liu Y, Wu J, Zou P (2019) Fluorometric determination of microRNA by using target-triggered cascade signal amplification and DNA-templated silver nanoclusters. Microchim Acta 186(10):669. https://doi.org/10.1007/s00604-019-3789-7
16. Wang Y, Shi H, Cui K, Zhang L, Ge S, Yan M, Yu J (2018) Hierarchical hematite/TiO_2 nanorod arrays coupled with responsive mesoporous silica nanomaterial for highly sensitive photoelectrochemical sensing. Biosens Bioelectron 117:515–521. https://doi.org/10.1016/j.bios.2018.06.030
17. Wang M, Yin H, Zhou Y, Han J, He T, Cui L, Ai S (2018) Photoelectrochemical biosensor for microRNA detection based on multiple amplification strategies. Microchim Acta 185(5):257. https://doi.org/10.1007/s00604-018-2808-4
18. Liu C, Zhao L, Liang D, Zhang X, Song W (2019) An $CuInS_2$ photocathode for the sensitive photoelectrochemical determination of microRNA-21 based on DNA–protein interaction and exonuclease III assisted target recycling amplification. Microchim Acta 186(11):692. https://doi.org/10.1007/s00604-019-3804-z
19. Liu G, Hong J, Ma K, Wan Y, Zhang X, Huang Y, Kang K, Yang M, Chen J, Deng S (2020) Porphyrin Trio−Pendant fullerene guest as an in situ universal probe of high ECL efficiency for sensitive miRNA detection. Biosens Bioelectron 150:111963. https://doi.org/10.1016/j.bios.2019.111963
20. Li Z, Lin Z, Wu X, Chen H, Chai Y, Yuan R (2017) Highly efficient electrochemiluminescence resonance energy transfer system in one nanostructure: its application for ultrasensitive detection of

microRNA in cancer cells. Anal Chem 89(11):6029–6035. https://doi.org/10.1021/acs.analchem.7b00616
21. Zhang R, Chen A, Yu Y, Chai Y, Zhuo Y, Yuan R (2018) Electrochemiluminescent carbon dot-based determination of microRNA-21 by using a hemin/G-wire supramolecular nanostructure as co-reaction accelerator. Microchim Acta 185(9):432. https://doi.org/10.1007/s00604-018-2959-3
22. Zhong X, Li X, Zhuo Y, Chai Y, Yuan R (2020) Synthesizing anode electrochemiluminescent self-catalyzed carbon dots-based nanocomposites and its application in sensitive ECL biosensor for microRNA detection. Sensor Actuat B-Chem 305:127490. https://doi.org/10.1016/j.snb.2019.127490
23. Shao H, Lu J, Zhang Q, Hu Y, Wang S, Guo Z (2018) Ruthenium-based metal organic framework (Ru-MOF)-derived novel Faraday-cage electrochemiluminescence biosensor for ultrasensitive detection of miRNA-141. Sensor Actuat B-Chem 268:39–46. https://doi.org/10.1016/j.snb.2018.04.088
24. Piñeiro Y, Buceta D, Calvo J, Huseyinova S, Cuerva M, Pérez Á, Domínguez B, López-Quintela MA (2015) Large stability and high catalytic activities of sub-nm metal (0) clusters: implications into the nucleation and growth theory. J Colloid Interf Sci 449:279–285. https://doi.org/10.1016/j.jcis.2015.01.001
25. Watanabe K, Welling TAJ, Sadighikia S, Ishii H, Imhof A, van Huis MA, van Blaaderen A, Nagao D (2020) Compartmentalization of gold nanoparticle clusters in hollow silica spheres and their assembly induced by an external electric field. J Colloid Interf Sci 566:202–210. https://doi.org/10.1016/j.jcis.2020.01.094
26. Mandal S, Wang J, Winans RE, Jensen L, Sen A (2013) Quantum size effects in the optical properties of ligand stabilized aluminum nanoclusters. J Phys Chem C 117(13):6741–6746. https://doi.org/10.1021/jp310514z
27. Chen A, Ma S, Zhuo Y, Chai Y, Yuan R (2016) In situ electrochemical generation of electrochemiluminescent silver naonoclusters on target-cycling synchronized rolling circle amplification platform for microRNA detection. Anal Chem 88(6):3203–3210. https://doi.org/10.1021/acs.analchem.5b04578
28. Yang H-Y, Wang H-J, Xiong C-Y, Chai Y-Q, Yuan R (2017) Intramolecular self-enhanced nanochains functionalized by an electrochemiluminescence reagent and its immunosensing application for the detection of urinary β2-microglobulin. ACS Appl Mater Inter 9(41):36239–36246. https://doi.org/10.1021/acsami.7b12011
29. Irkham WT, Fiorani A, Valenti G, Paolucci F, Einaga Y (2016) Co-reactant-on-demand ECL: Electrogenerated chemiluminescence by the in situ production of $S_2O_8^{2-}$ at boron-doped diamond electrodes. J Am Chem Soc 138(48):15636–15641. https://doi.org/10.1021/jacs.6b09020
30. Lei Y-M, Wen R-X, Zhou J, Chai Y-Q, Yuan R, Zhuo Y (2018) Silver ions as novel coreaction accelerator for remarkably enhanced electrochemiluminescence in a PTCA–$S_2O_8^{2-}$ system and its application in an ultrasensitive assay for mercury ions. Anal Chem 90(11):6851–6858. https://doi.org/10.1021/acs.analchem.8b01018
31. Ma M-N, Zhuo Y, Yuan R, Chai Y-Q (2015) New signal amplification strategy using semicarbazide as co-reaction accelerator for highly sensitive electrochemiluminescent aptasensor construction. Anal Chem 87(22):11389–11397. https://doi.org/10.1021/acs.analchem.5b02848
32. Sun Y, Wu X, Zhang K, Ren Q, Xie R (2018) Electrochemiluminescent quaternary Cu-Zn-In-S nanocrystals as a sensing platform: enzyme-free and sensitive detection of the FLT3 gene based on triple signal amplification. Biosens Bioelectron 100:445–452. https://doi.org/10.1016/j.bios.2017.09.026
33. Dong X, Zhao G, Li X, Miao J, Fang J, Wei Q, Cao W (2019) Electrochemiluminescence immunoassay for the N-terminal pro-B-type natriuretic peptide based on resonance energy transfer between a self-enhanced luminophore composed of silver nanocubes on gold nanoparticles and a metal-organic framework of type MIL-125. Microchim Acta 186(12):811. https://doi.org/10.1007/s00604-019-3969-5
34. Feng L, Wu L, Xing F, Hu L, Ren J, Qu X (2017) Novel electrochemiluminescence of silver nanoclusters fabricated on triplex DNA scaffolds for label-free detection of biothiols. Biosens Bioelectron 98:378–385. https://doi.org/10.1016/j.bios.2017.07.016
35. Chen Y, Zhou Y, Yin H, Li F, Li H, Guo R, Han Y, Ai S (2020) Photoelectrochemical biosensor for histone acetyltransferase detection based on ZnO quantum dots inhibited photoactivity of BiOI nanoflower. Sensor Actuat B-Chem 307:127633. https://doi.org/10.1016/j.snb.2019.127633
36. Bhardwaj SK, Bhardwaj N, Mohanta GC, Kumar P, Sharma AL, Kim K-H, Deep A (2015) Immunosensing of atrazine with antibody-functionalized Cu-MOF conducting thin films. ACS Appl Mater Inter 7(47):26124–26130. https://doi.org/10.1021/acsami.5b07692
37. Wang H, Jian Y, Kong Q, Liu H, Lan F, Liang L, Ge S, Yu J (2018) Ultrasensitive electrochemical paper-based biosensor for microRNA via strand displacement reaction and metal-organic frameworks. Sensor Actuat B-Chem 257:561–569. https://doi.org/10.1016/j.snb.2017.10.188
38. Miao P, Wang B, Chen X, Li X, Tang Y (2015) Tetrahedral DNA nanostructure-based microRNA biosensor coupled with catalytic recycling of the analyte. ACS Appl Mater Inter 7(11):6238–6243. https://doi.org/10.1021/acsami.5b01508
39. Lv W, Zhao J, Situ B, Li B, Ma W, Liu J, Wu Z, Wang W, Yan X, Zheng L (2016) A target-triggered dual amplification strategy for sensitive detection of microRNA. Biosens Bioelectron 83:250–255. https://doi.org/10.1016/j.bios.2016.04.053
40. Wang B, Dong Y-X, Wang Y-L, Cao J-T, Ma S-H, Liu Y-M (2018) Quenching effect of exciton energy transfer from CdS:Mn to Au nanoparticles: a highly efficient photoelectrochemical strategy for microRNA-21 detection. Sens. Actuators B 254:159–165. https://doi.org/10.1016/j.snb.2017.07.078
41. Zhu H-Y, Ding S-N (2019) Dual-signal-amplified electrochemiluminescence biosensor for microRNA detection by coupling cyclic enzyme with CdTe QDs aggregate as luminophor. Biosens Bioelectron 134:109–116. https://doi.org/10.1016/j.bios.2019.04.005
42. Lu L, Liu C, Kang T, Wang X, Guo G, Miao W (2018) In situ enhanced electrochemiluminescence based on co-reactant self-generated for sensitive detection of microRNA. Sensor Actuat B-Chem 255:35–41. https://doi.org/10.1016/j.snb.2017.08.029
43. Fu R, Zhang M, Zhao Y, He X, Ding C, Wang S, Feng Y, Song X, Li P, Wang B (2017) Identification of salt tolerance-related microrna and their targets in maize (Zea mays L.) using high-throughput sequencing and degradome analysis. Front Plant Sci 8:864
44. Kong X, Zhang M, Xu X, Li X, Li C, Ding Z (2014) System analysis of microRNAs in the development and aluminium stress responses of the maize root system. Plant Biotechnol J 12(8):1108–1121. https://doi.org/10.1111/pbi.12218
45. Wu Y, Guo J, Cai Y, Gong X, Xiong X, Qi W, Pang Q, Wang X, Wang Y (2016) Genome-wide identification and characterization of Eutrema salsugineum microRNAs for salt tolerance. Physiol Plantarum 157(4):453–468. https://doi.org/10.1111/ppl.12419